

## Reactive molecular dynamics simulation of early stage of dry oxidation of Si (100) surface

Mauludi Ariesto Pamungkas,<sup>1,2</sup> Minwoong Joe,<sup>1</sup> Byung-Hyun Kim,<sup>1,3</sup> and Kwang-Ryeol Lee<sup>1,2,a)</sup>

<sup>1</sup>Computational Science Center, Korea Institute of Science and Technology, 39-1, Hawolgok-dong, Seongbuk-gu, Seoul 136-791, Korea

<sup>2</sup>Nanomaterial Science and Technology, University of Science and Technology, 113 Gwahangno, Yuseong-gu, Daejeon, Korea

<sup>3</sup>Division of Materials Science and Engineering, Hanyang University, Seoul 133-791, Korea

(Received 1 June 2011; accepted 23 July 2011; published online 9 September 2011)

Initial stage of oxidation of Si (100) surface by O<sub>2</sub> molecules was investigated in atomic scale by molecular dynamics (MD) simulation at 300 K and 1200 K without external constraint on the oxygen molecules. A reactive force field was used for the simulation to handle charge variation as well as breaking and forming of the chemical bonds associated with the oxidation reaction. Results of the present simulation are in good agreement with previous first principle calculations and experimental observations: the oxygen molecules spontaneously dissociated on the Si (100) surface and reacted with Si first layer without energy barrier. The simulation also exhibited that the reacted oxygen preferentially located in the back bonds of the surface dimer. Consecutive oxidation simulation with 300 O<sub>2</sub> molecules showed that the diffusion of oxygen atom into the subsurface of clean Si surface can occur during very short time of the present oxidation simulation. The present MD simulation also revealed that the oxidation at 300 K results in more stoichiometric oxide layer than that at 1200 K. © 2011 American Institute of Physics. [doi:10.1063/1.3632968]

### INTRODUCTION

Silicon oxide (SiO<sub>x</sub>) has been adapted to the gate dielectric material of complementary metal oxide semiconductor (CMOS) transistor owing to its thermodynamic stability, excellent interface with a few defects, and superior electrical isolation properties. For last decades, scaling of Si CMOS device has proceeded with the reduction in the thickness of the SiO<sub>x</sub> dielectric layer to a few atomic layers.<sup>1,2</sup> Engineering the interface structure between Si and the extremely thin SiO<sub>x</sub> has been thus considered as an essential factor in the device performance, leading to the requirement of an atomic scale understanding in the early stage of Si oxidation. Therefore, the initial stage of Si oxidation has been one of the most intensively studied topics, yet remains controversial. Even in the high-*k* dielectric gate stack for future devices, the formation of very thin SiO<sub>x</sub> layer at the interface is essential to minimize the interface state density.<sup>3–5</sup> Therefore, understanding the initial stage of Si oxidation is still relevant and crucial to optimize the gate structure of next generation devices. Initial oxidation behavior also attracts much attention due to its unique features that cannot be well described by the classical kinetic models.<sup>6–9</sup>

A great deal of experimental investigation has been performed to resolve the oxidation state of the Si atoms in molecular level using various experimental techniques such as surface differential reflectance (SDR),<sup>10,11</sup> x-ray or ultraviolet photoemission spectroscopy (XPS/UPS),<sup>8,12–15</sup> scanning reflection electron microscopy (SREM),<sup>16</sup> *in situ* Auger electron spectroscopy (AES) combined with reflection high

energy electron diffraction (RHEED),<sup>17</sup> high resolution Rutherford backscattering spectrometry (HRBS),<sup>18</sup> or scanning tunneling microscope (STM).<sup>6,19,20</sup> However, the experimental observations exhibited complex behaviors of the initial oxidation phenomena, and the atomic scale computation has been expected to provide deeper insight of the reaction. Many theoretical calculations using density functional theory revealed the most probable oxygen adsorption path by comparing the energy barriers of several possible paths.<sup>21–27</sup> Direct oxidation simulation using quantum molecular dynamics was also tried to understand kinetic pathway for Si oxidation.<sup>27–31</sup> *Ab initio* or classical MD simulations were employed to find the structural model of Si/SiO<sub>x</sub> interface using an artificially built interface as the starting materials or inserting O in Si-Si network.<sup>4,32–37</sup> Because the *ab initio* MD simulations were limited in both time scale and the size of the calculation system, the previous works could not extend beyond single O<sub>2</sub> molecule reaction on a small Si (100) dimer configuration. The classical MD simulations were also performed under the constrained condition where the oxygen atoms were impinged into Si-Si bond at the interface followed by relaxation.<sup>33,34,38,39</sup> Although the previous theoretical works enabled the atomistic understanding of the structures of the oxide layer itself or its interface with Si, it is still far from understanding the Si oxidation behavior during real oxidation process.

In the present work, we tried to simulate the oxidation behavior of Si (100) surface by placing oxygen molecules on the Si (100) surface at an oxidation temperature without any external constraint on the oxygen molecule. We investigated the oxidation by a reactive molecular dynamics simulation method using the reactive force field (ReaxFF) of Si-O

<sup>a)</sup>Electronic mail: krlee@kist.re.kr.

system developed by van Duin *et al.*<sup>40</sup> The simulated single O<sub>2</sub> molecule reaction exhibited the behaviors consistent with the previous theoretical works, which validates the ReaxFF for the MD simulation in more realistic oxidation condition. Consecutive oxidation simulation using 300 O<sub>2</sub> molecules showed that in the initial stage of oxidation, more stoichiometric oxide surface can be formed at 300 K, whereas broad sub-oxide surface was formed at 1200 K. This result would result from considerable oxygen diffusion into the clean Si matrix even in the time scale of a few ns.

### Computation details

Surface oxidation of Si needs an interatomic potential that can provide consistent description appropriate for covalent system of Si and all forms of ionic silicon oxide systems. The potential function should also correctly handle the charge distribution (or reaction) between oxygen and silicon. We used the ReaxFF for Si-O system, which would allow accurate simulations of the bond breaking during oxidation and the interface evolution between silica and silicon.<sup>40</sup> The system energy in the ReaxFF is partitioned into several partial energy contributions. All the covalent interaction terms are expressed by the continuously updated bond order. The bond order is calculated from the instantaneous interatomic distance to allow the creation and dissociation of bonds during a simulation. The interactions are then formulated to ensure that their energy contributions disappear upon bond dissociation. Because bonds are breaking and reforming during dynamic simulations, pairwise nonbonding interactions such as van der Waals and Coulomb interactions are also included for all atom pairs. For the Coulomb interaction, atomic charges are calculated using the electron equilibration method (EEM). EEM parameters were optimized using Mulliken charge distribution obtained by density functional theory calculations.

“Large-scale Atomic/Molecular Massively Parallellized Simulator” (LAMMPS) code integrated with ReaxFF was used for the present simulations.<sup>41</sup> The ReaxFF integrated in LAMMPS was benchmarked with amorphous silica, since the oxidation of Si surface results in an amorphous SiO<sub>x</sub> layer. Amorphous SiO<sub>2</sub> was constructed by initially heating an  $\alpha$ -quartz up to 6000 K in isobaric-isothermal microensemble ensemble until the system was completely melted and quenching the melt to room temperature within 1 ps. Figure 1 shows the partial radial distribution function (p-RDF) of the amorphous silica and Table I, the density and atomic bond structure obtained from the amorphous SiO<sub>2</sub>. Partial RDF spectrum is almost identical to that obtained by Fogarty *et al.*<sup>42</sup> using another ReaxFF implementation (SERIALREAX). (See Fig. 7 in Ref. 42.) Vashishita *et al.*<sup>43</sup> also reported the narrow Si-Si partial RDF spectrum. Because the simulated spectrum was obtained without considering the finite detector resolution of the experiment, only the mean values of the peak position can be compared with the experimental measurements. As shown in Table I, all the calculated structural characteristics of amorphous SiO<sub>2</sub> are in good agreement with the experimental measurements.

Figure 2(a) shows the simulation box for the present simulation. Slab model of single crystal Si of (100) surface

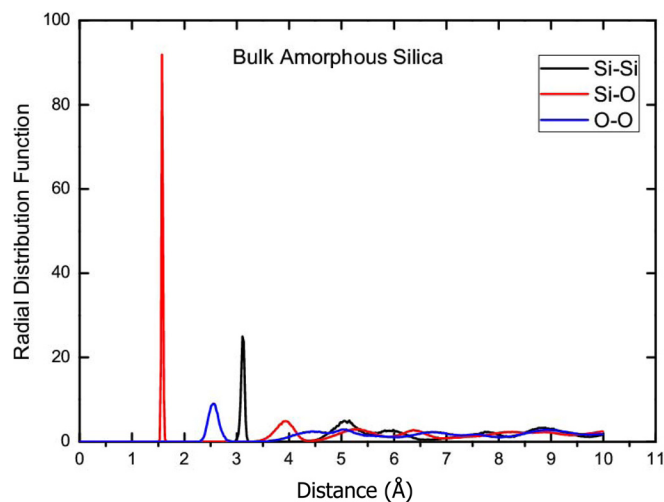


FIG. 1. (Color online) p-RDF of amorphous silica.

was used as the substrate after relaxing at 300 K for 10 ps. Figure 2(b) shows the topview of the Si surface which exhibits the well-known surface dimers along  $\langle 110 \rangle$  direction as marked by white lines. Reasonable agreement between calculated and observed properties of crystalline Si was also obtained as summarized in Table II. In order to mimic a thick substrate, Si atoms in the bottom 0.1 nm region of the simulation box was fixed. Atoms in the region of about 6.6 nm above the fixed layer were kept at a constant oxidation temperature (300 K or 1200 K) during simulation to provide a thermal bath in the system. Temperature of the thermal bath was rescaled at every time step (1 fs) during simulations. All the atoms above the thermal bath were unconstrained with an initial temperature set to the oxidation temperature. Oxidation simulation was done by placing an O<sub>2</sub> molecule presented by blue balls (indicated by an arrow in Figs. 2(a) and 2(b)) at the distance 0.12 nm above the surface, without any external constraint. This distance was chosen from the preliminary simulation to find the largest distance for the O<sub>2</sub> molecule to react with Si surface. Two simulation sets were carried out. In order to compare the oxidation behavior with the previous *ab initio* calculations or the experimental results of surface reaction, single O<sub>2</sub> molecule reactions were investigated on randomly selected surface positions with various oxygen molecule configurations for 10 ps. 1000 independent single molecular reactions were statistically analyzed. Second, we oxidized the surface by

TABLE I. Structural properties of amorphous silica calculated by molecular dynamics using ReaxFF and experimentally observed data.

	ReaxFF MD	Experiment
Density (g/cm <sup>3</sup> )	2.25	2.20 <sup>a</sup>
O-Si-O angle (°)	109.36	109.4 <sup>a</sup>
Si-O-Si angle (°)	142	144 <sup>a</sup>
Si-Si distance (nm)	0.310 ± 0.02	0.3077, 0.312 <sup>a</sup>
O-O distance (nm)	0.270 ± 0.04	0.2626, <sup>b</sup> 0.265 <sup>a</sup>
Si-O distance (nm)	0.159 ± 0.006	0.1608, <sup>b</sup> 0.1620 <sup>a</sup>

<sup>a</sup>Reference 49.

<sup>b</sup>Reference 50.

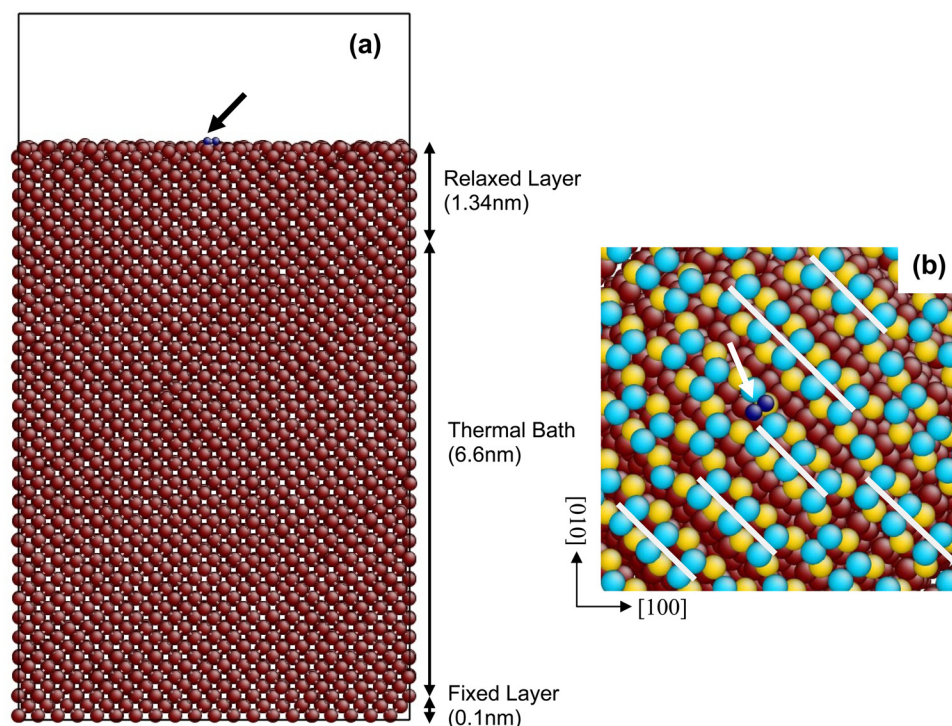


FIG. 2. (Color online) Side (a) and top view(b) of the simulation box.

sequentially adding 300  $O_2$  molecules on the surface to study the oxide surface layer evolution.

## RESULTS AND DISCUSSION

Figure 3 shows the typical snapshots of the oxidation reaction when the oxygen molecule was placed on the dimer row of the relaxed Si (100) surface at 300 K (Figs. 3(a)–3(c)) and 1200 K (Figs. 3(d)–3(f)). Three different configurations of oxygen molecule with respect to the surface were investigated:  $\theta = 90^\circ$  (Figs. 3(a) and 3(d)),  $45^\circ$  (Figs. 3(b) and 3(e)), and  $0^\circ$  (Figs. 3(c) and 3(f)), where  $\theta$  is the angle between the O–O axis in the oxygen molecule and the surface normal. When  $\theta = 90$  or  $45^\circ$ , most oxygen molecules spontaneously dissociated into two oxygen atoms in at most 100 fs at both 300 and 1200 K. This simulation results support the experimental observations that the first subsurface oxidation occurs without energy barrier.<sup>10,16</sup> The temperature independence of the dissociation behavior will be discussed later. After dissociation, the oxygen atoms formed silanone species on the surface as indicated by arrows in Figs. 3(a), 3(b) and 3(d). The silanone species as a stable intermediate phase of Si oxidation was suggested by both infrared absorption spectroscopy and the first-principles quantum chemical calculations combined

with STM study.<sup>26,44,45</sup> The oxygen atoms then rapidly moved from the dimer row position to the channel between the dimers in the direction opposite to each other. The opposite movement would be a natural consequence of Coulombic repulsion. Both oxygen atoms were then incorporated into the back bonds of the dimer row, in agreement with the previous experimental and theoretical results.<sup>5,11,16,23,24</sup> The oxygen-silicon reaction occurred almost spontaneously within 0.5 ps at both 300 K and 1200 K. The oxidation reaction was essentially same when  $\theta = 0^\circ$  (Fig. 3(c) or 3(f)), except that upper oxygen atom in the molecule frequently left from the surface after the dissociation.

The reaction kinetics is dependent on the position of oxygen molecule on the Si (100) surface. Figure 4 shows the oxidation process when the oxygen molecules were placed on the channel between dimmers. Because of the longer distance from the surface silicon atoms, dissociation of the oxygen molecule occurs more slowly than those in Fig. 3. However, the resulting atomic configuration of the oxygen incorporated Si surface is essentially the same.

The spontaneous dissociation of oxygen molecule observed in the present MD simulation is consistent with recent *ab initio* calculations.<sup>16,21,24,28,29,46</sup> Richard *et al.*<sup>46</sup> suggested the different barrierless pathways for the direct dissociation of the oxygen molecule, depending on the initial position of the molecule. They showed that low activation barrier (0.25 eV) for the dissociation of oxygen molecule can be readily overcome by the energy gain of the dimer-breaking accompanied with the chemisorption of the oxygen molecule. The *ab initio* calculation revealed that the dissociation of oxygen molecule on Si surface lower the energy by 4.14 eV. This energy gain will generate “hot atoms” that can provide enough kinetics for the oxygen incorporation into the back bonds of Si dimer. The hot atom mechanism would

TABLE II. Properties of crystalline Si calculated by molecular statics using ReaxFF, calculated by *ab initio* density functional theory and experimentally observed data.

Silicon	ReaxFF MD	AB Initio <sup>c</sup>	Exp <sup>c</sup>
Lattice constant (nm)	0.532	0.545	0.543
Bulk modulus (Mbar)	1.12	0.98	0.99
Cohesive energy (eV/atom)	4.56	4.84	4.63

<sup>c</sup>Reference 51 and references therein.

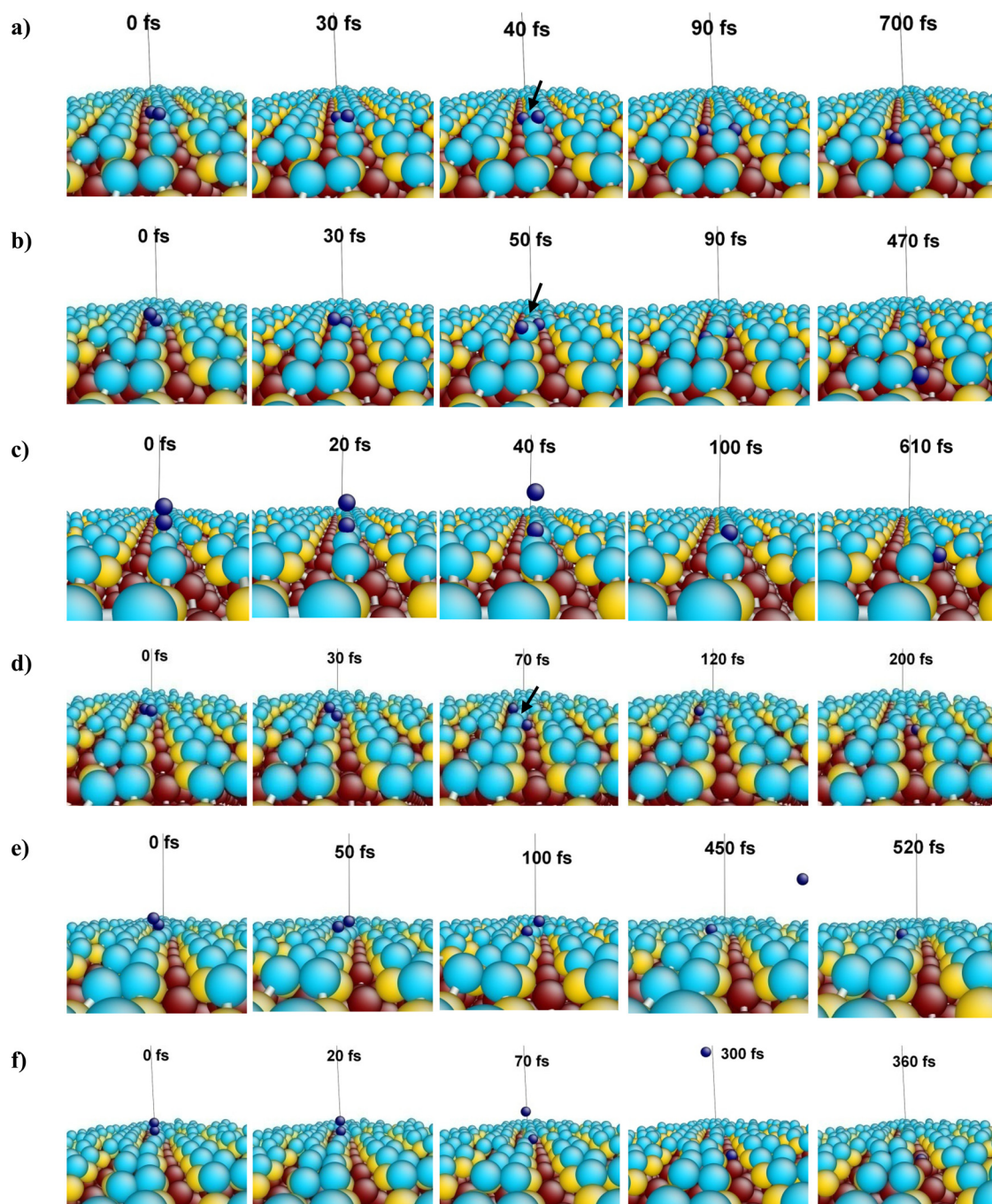


FIG. 3. (Color online) Time evolution of single oxygen molecule reaction at 300 K for (a)  $\theta = 90^\circ$ , (b)  $45^\circ$ , and (c)  $0^\circ$ . Time evolutions at 1200 K are shown in (c), (d) and (e) for  $\theta = 90^\circ$ ,  $45^\circ$  and  $0^\circ$ , respectively.

explain the similar behavior of oxygen reaction regardless of the oxidation temperature.

For a statistical analysis of the oxygen-silicon interaction, we performed simulations of 1000 independent single

$O_2$  molecule reactions for 10 ps with randomly placing an oxygen molecule on the Si (100) surface. We observed that the system energy fluctuation due to the oxygen incorporation is pacified after 3 ps. Table III shows the probability of an

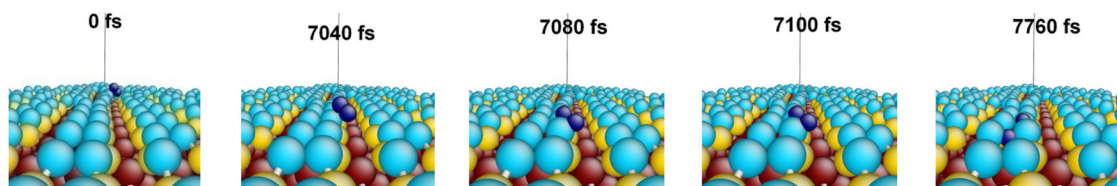


FIG. 4. (Color online) Time evolution of single oxygen molecule reaction when oxygen molecule is placed on a channel of dimer rows at 300 K with  $\theta = 45^\circ$ .

TABLE III. Total uptake fraction of oxygen and the depth distribution of the oxygen obtained by statistical analysis of 1000 single O<sub>2</sub> reaction events.

Oxygen position after 10 ps	300 K	1200 K
Layer 1 (0.0-0.2 nm)	70.76%	69.47%
Layer 2 (0.2-0.4 nm)	20.63%	21.73%
Layer 3 (0.4-0.6 nm)	8.23%	7.81%
Layer 4 (0.6-0.8 nm)	0.37%	0.85%
Layer 5 (0.8-1.0 nm)	0%	0.13%
Total fraction of adsorbed oxygen	80.20%	76.15%

oxygen atom to be placed in a certain depth. Because of the time limit of the MD simulation, the probability was obtained without considering the thermal diffusion in long time scale. Therefore, the depth profile data of Table III would be steeper than in real oxidation reaction and the discrepancy will be more significant at higher oxidation temperature. In spite of the limitation in time scale, it is evident that the oxygen atom significantly penetrated into the Si matrix at both 300 and 1200 K. Considering the present simulation time of 10 ps, the diffusion in this simulation would be the ballistic one as proposed by Yasuda *et al.*<sup>10</sup> Slightly higher probability of oxygen in deep layer 5 (0.8~1.0 nm in depth) was observed in 1200 K simulation. The total fraction of oxygen atoms incorporated into Si substrate is also dependent on the oxidation temperature: about 19.8% and 23.85% of oxygen atoms left the Si surface at 300 K and 1200 K, respectively. Figures 3(c), 3(e), and 3(f) show the cases that one of the oxygen atoms left the Si surface after dissociation of O<sub>2</sub> molecule. At

higher temperature, larger kinetic energy of the oxygen molecule would increase the probability for the oxygen atom to leave without reaction. However, it must be noted that the difference in the fraction is not as significant as the difference in the oxidation temperature. This result implies that the oxidation reaction on Si (100) surface is more dependent on the initial configuration than the oxidation temperature, which would be caused by the low energy barrier for the dissociation of the oxygen molecule.<sup>16,21,24,28,29,46</sup> The single O<sub>2</sub> molecule reaction simulations using the ReaxFF were in good agreement with the previous experimental and theoretical works, which support that the ReaxFF represents well the oxidation behavior of the Si surface.

Next, we simulated the oxidation of the Si (100) surface by consecutively supplying 300 oxygen molecules on randomly selected position of the surface with randomly chosen angle  $\theta$ . The interval between two consecutive addition of the oxygen molecule was set to be 20 ps. Total simulation time was thus 6 ns. Before supplying each oxygen molecule, temperature of the system was rescaled to the oxidation temperature. It must be noted that the present work would reveal the initial oxidation behavior of clean Si (100) surface, because the time scale of the present simulation is not enough to consider the thermal diffusion of oxygen in long time scale. Figure 5(a) shows the atomic configuration of the oxidized surface. Oxygen atom is presented by blue balls while silicon by dark brown ones. It appeared that the atomic structure of the surface became amorphous by the oxidation. We calculated the radial distribution function (RDF) of the

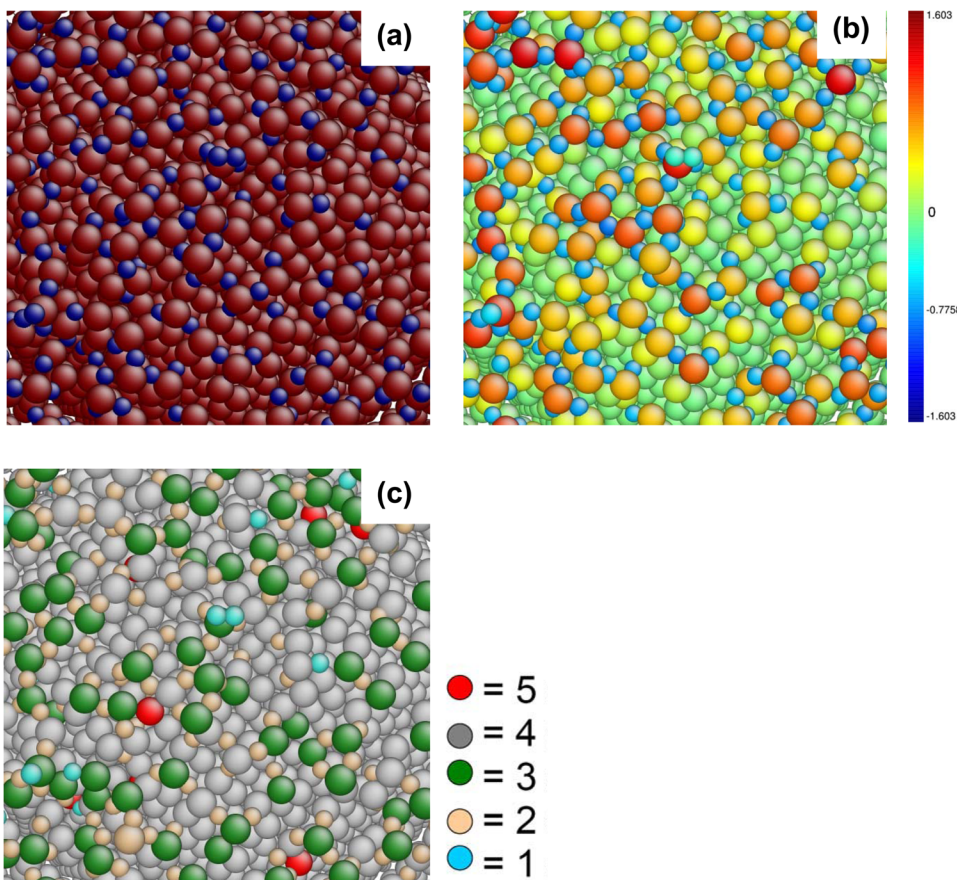


FIG. 5. (Color online) Top view of the oxidized surface by 300 oxygen molecules consecutively added on the surface every 20 ps. The atoms are colored by (a) the atom (oxygen in dark blue and silicon in dark brown) (b) the Mulliken charge as shown in the color index bar, and (c) the coordination number.

oxidized surface layer of thickness 1.37 nm. Even if the RDF was of large statistical noise, it was evident that no long range order was observed. The distances of the first nearest neighbor of Si-O and O-O bonds are in good agreement with those of the amorphous SiO<sub>2</sub> (Fig. 1). However, the first nearest neighbor distance of Si-Si bonds is closer to the crystalline Si because the present simulation was in the sub-oxide formation regime.

Figure 5(b) shows the charge distribution on the oxidized surface. Color scale in Fig. 5(b) represents the range of the Mulliken charge values. The snapshot evidently showed that the electrons transferred from silicon to oxygen during oxidation reaction. It was also noted that the charge transfer only occurred between silicon and the nearest oxygen atoms. Charge of Si increased with the number of nearest oxygen atoms, with the maximum of 1.60e when three oxygen atoms are in the nearest neighbor. This value is equivalent to that of silicon dioxide.<sup>40</sup> Colors in Fig. 5(c) represent the coordination number of the atoms. The coordination number was estimated by the number of atoms within the radius of 0.35 nm. In the surface region, coordination number of Si ranged from 2 to 5 implying that the structural property of crystalline surface was lost by the oxidation. Most Si atoms are 3 or 4 coordinated, whereas most oxygen atoms agglomerate around Si atoms with the coordination number of 2.<sup>14,27,47</sup>

Initial oxidation behaviors at 300 K and 1200 K were compared by analyzing the simulated oxide layer. Figure 6 shows the oxygen depth profile after the simulation. The oxygen profiles are notably dependent on the oxidation temperature. At 300 K, oxygen atoms were accumulated on the surface layer. On the other hand, oxygen atoms penetrated into deeper layer at 1200 K resulting in broad distribution of oxygen. This difference would be a natural consequence of the increased kinetic energy of oxygen that enhances the atomic movement into Si network. This oxygen profile is in contrast to the layer-by-layer growth model.<sup>12,33,34</sup> However, the present simulation is consistent with oxygen depth profiles obtained by high resolution XPS analysis of Si/SiO<sub>x</sub>

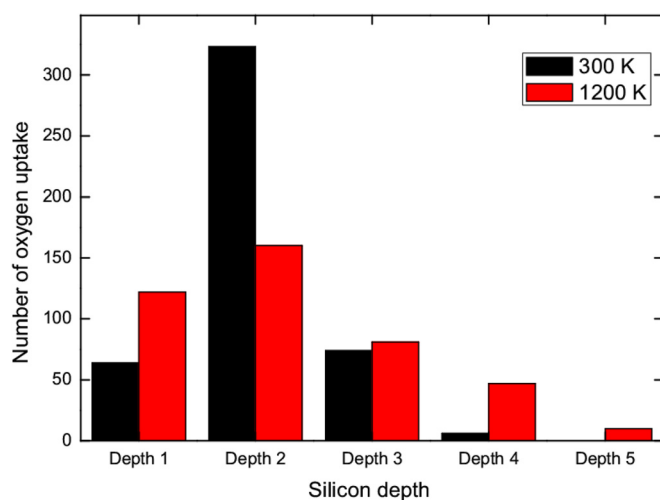


FIG. 6. (Color online) Oxygen depth profile of the oxidized silicon surface after consecutive oxidation reactions with 300 oxygen molecules. Each data was taken in the layer of thickness 0.3 nm from the surface. Because of increased surface roughness by oxidation, data in depth 1 is undependable.

interface,<sup>15</sup> HRBS spectra,<sup>18</sup> and classical MD simulation of Si/SiO<sub>x</sub> interface.<sup>38</sup>

The oxygen composition profile should affect the stoichiometry of the evolved oxide layer. Figure 7 shows the time evolution of Si<sup>+</sup>, Si<sup>2+</sup>, Si<sup>3+</sup>, and Si<sup>4+</sup> ion fraction in the specimen during oxidation simulation. Charge state of Si was determined by the number of nearest oxygen atoms, as suggested by the calculated core shifts in Si-SiO<sub>2</sub> interface.<sup>48</sup> At 300 K, number of Si<sup>+</sup> monotonically decreased as the oxidation proceeded while those of Si<sup>2+</sup>, Si<sup>3+</sup>, and Si<sup>4+</sup> increased (See Fig. 7(a)). The oxygen atoms accumulated on the surface layer at 300 K (as shown in Fig. 6) can generate a stoichiometric surface oxide layer. Even in the present simulation of early stage of Si oxidation, we could observe that Si<sup>3+</sup> or Si<sup>4+</sup> ions are accumulated in the surface layer. Recently, *in situ* experimental observation of the oxidized Si (100) surface also reported that the 1st layer is fully oxidized at room temperature oxidation.<sup>5</sup> Fig. 7(b) shows the time evolution of Si ion fraction during 1200 K oxidation simulation. It can be noted that more than 50% of the Si ions remained as Si<sup>+</sup> while the fraction of Si<sup>4+</sup> was less than 5%.

In the present oxidation simulation, total simulation time was just 6 ns. Therefore, it must be noted that the present simulations are applied only for very initial stage of the

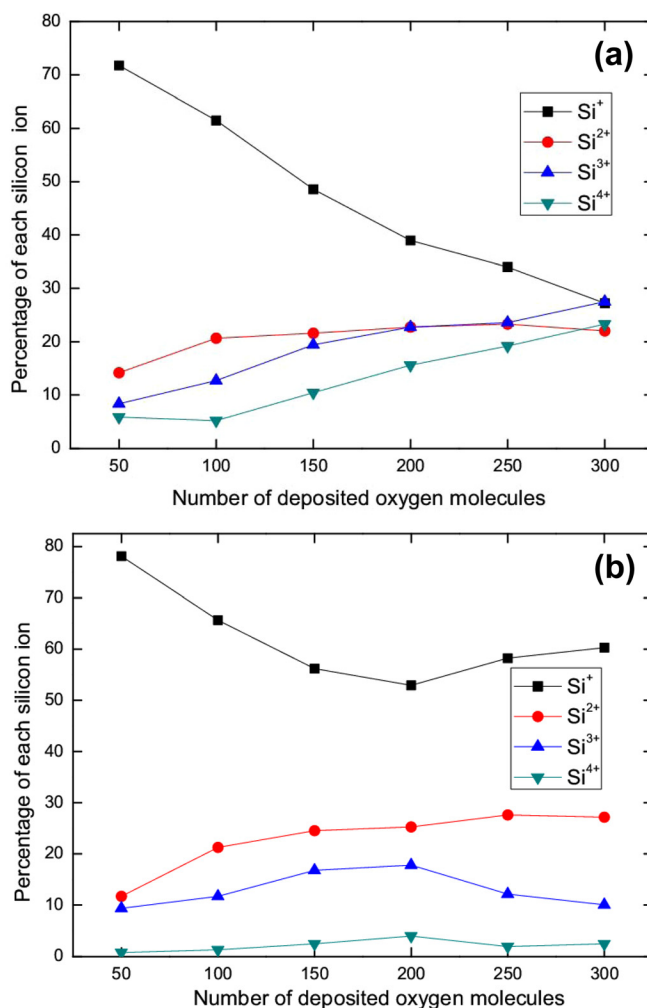


FIG. 7. (Color online) Time evolution of the charge state of silicon during consecutive oxidation simulation at (a) 300 K and (b) 1200 K.

oxidation and exclude thermal diffusion of oxygen in long time scale. In spite of this limitation, the present results show that the difference in the oxygen depth profile between the processes at 300 and 1200 K can be evolved in early stage of oxidation. In real oxidation process, where thermal diffusion of oxygen can occur during oxidation, the difference in the oxidation behaviors at two different temperatures would be more significant than the present simulation results. From this simulation results, it can be said that the ambient oxidation of clean Si (001) surface at 300 K will result in better quality of oxide surface. In the later stage, where the oxidation is governed by oxygen diffusion via oxide layer, high temperature oxidation will result in faster kinetics of the oxidation process.

## CONCLUSION

The present work showed the viability of the reactive MD technique for a massive simulation of Si oxidation in atomic scale without external constraint on the oxygen molecule, which would overcome the limits of the previous constrained oxidation simulations. Reactive MD simulations of early stage of dry oxidation of Si (100) surface using the reactive force field of Si-O system revealed the reaction behaviors in atomic scale which are in good agreement with the previous experimental and *ab initio* calculation results. The simulation of single oxygen molecule reaction confirmed typical phenomena in silicon oxidation process such as dissociative adsorption, silanone precursor of oxidation, oxygen agglomeration, and ion silicon transformation. Furthermore, consecutive oxidation simulation for 6 ns exhibited the initial evolution of the surface oxide layer. At the oxidation temperature of 1200 K, significant sub-oxide layer was formed during the simulation for 6 ns, whereas the simulation at 300 K showed the surface layer evolution to form more stoichiometric SiO<sub>2</sub> layer.

## ACKNOWLEDGMENTS

This research was supported by the Converging Research Center Program through Korea Ministry of Education, Science and Technology (2010K000992).

<sup>1</sup>A. I. Kingon, J. P. Maria, and S. K. Streiffer, *Nature* **406**, 1032 (2000).

<sup>2</sup>Y. P. Lin and J. G. Hwu, *J. Vac. Sci. Technol. A* **22**, 2265 (2004).

<sup>3</sup>S. Sayan, E. Garfunkel, and S. Suzer, *Appl. Phys. Lett.* **80**, 2135 (2002).

<sup>4</sup>D. Fischer, A. Curioni, S. Billeter, and W. Andreoni, *Appl. Phys. Lett.* **88**, 012101 (2006).

<sup>5</sup>K. Gaal-Nagy, A. Incze, G. Onida, Y. Borensztein, N. Witkowski, O. Pluchery, F. Fuchs, F. Bechstedt, and R. Del Sole, *Phys. Rev. B* **79**, 045312 (2009).

<sup>6</sup>T. Engel, *Surf. Sci. Rep.* **18**, 91 (1993).

<sup>7</sup>T. Watanabe, K. Tatsumura, and I. Ohdomari, *Phys. Rev. Lett.* **96**, 196102 (2006).

<sup>8</sup>Y. Enta, B. S. Mun, M. Rossi, P. N. Ross, Z. Hussain, C. S. Fadley, K. S. Lee, and S. K. Kim, *Appl. Phys. Lett.* **92**, 012110 (2008).

<sup>9</sup>H. Cui, C. X. Wang, G. W. Yang, and D. Jiang, *Appl. Phys. Lett.* **93**, 203113 (2008).

<sup>10</sup>T. Yasuda, N. Kumagai, M. Nishizawa, S. Yamasaki, H. Oheda, and K. Yamabe, *Phys. Rev. B* **67**, 195338 (2003).

<sup>11</sup>S. Ohno, J. Takizawa, J. Koizumi, K. Shudo, and M. Tanaka, *J. Phys.: Condens. Matter* **19**, 446011 (2007).

<sup>12</sup>Y. Harada, M. Niwa, T. Nagatomi, and R. Shimizu, *Jpn. J. Appl. Phys.* **39**(1), 560 (2000).

<sup>13</sup>M. Suemitsu, Y. Enta, Y. Miyanishi, and N. Miyamoto, *Phys. Rev. Lett.* **82**, 2334 (1999).

<sup>14</sup>H. W. Yeom, H. Hamamatsu, T. Ohta, and R. I. G. Uhrberg, *Phys. Rev. B* **59**, 10413 (1999).

<sup>15</sup>J. H. Oh, H. W. Yeom, Y. Hagimoto, K. Ono, M. Oshima, N. Hirashita, M. Nywa, A. Toriumi, and A. Kakizaki, *Phys. Rev. B* **63**, 205310 (2001).

<sup>16</sup>H. Watanabe, K. Kato, T. Uda, K. Fujita, M. Ichikawa, T. Kawamura, and K. Terakura, *Phys. Rev. Lett.* **80**, 345 (1998).

<sup>17</sup>Y. Takakuwa, F. Ishida, and T. Kawawa, *Appl. Surf. Sci.* **216**, 133 (2003).

<sup>18</sup>K. Nakajima, Y. Okazaki, and K. Kimura, *Phys. Rev. B* **63**, 113314 (2001).

<sup>19</sup>C. H. Chung, H. W. Yeom, B. D. Yu, and I. W. Lyo, *Phys. Rev. Lett.* **97**, 036103 (2006).

<sup>20</sup>H. Itoh, K. Nakamura, A. Kurokawa, and S. Ichimura, *Surf. Sci.* **482**, 114 (2001).

<sup>21</sup>Y. Miyamoto and A. Oshiyama, *Phys. Rev. B* **41**, 12680 (1990).

<sup>22</sup>Y. Miyamoto and A. Oshiyama, *Phys. Rev. B* **43**, 9287 (1991).

<sup>23</sup>K. Kato, T. Uda, and K. Terakura, *Phys. Rev. Lett.* **80**, 2000 (1998).

<sup>24</sup>K. Kato and T. Uda, *Phys. Rev. B* **62**, 15978 (2000).

<sup>25</sup>X. L. Fan, Y. F. Zhang, W. M. Lau, and Z. F. Liu, *Phys. Rev. Lett.* **94**, 016101 (2005).

<sup>26</sup>A. Hemeryck, A. Esteve, N. Richard, M. D. Rouhani, and Y. J. Chabal, *Phys. Rev. B* **79**, 035317 (2009).

<sup>27</sup>A. Pasquarello, M. S. Hybertsen, and R. Car, *Nature* **396**, 58 (1998).

<sup>28</sup>A. Bongiorno and A. Pasquarello, *Phys. Rev. Lett.* **93**, 086102 (2004).

<sup>29</sup>L. C. Ciacchi and M. C. Payne, *Phys. Rev. Lett.* **95**, 196101 (2005).

<sup>30</sup>T. Uchiyama and M. Tsukada, *Phys. Rev. B* **53**, 7917 (1996).

<sup>31</sup>T. Uchiyama and M. Tsukada, *Phys. Rev. B* **55**, 9356 (1997).

<sup>32</sup>A. Pasquarello, M. S. Hybertsen, and R. Car, *Phys. Rev. Lett.* **74**, 1024 (1995).

<sup>33</sup>T. Watanabe, K. Tatsumura, and I. Ohdomari, *Appl. Surf. Sci.* **237**, 125 (2004).

<sup>34</sup>P. Ganster, G. Treglia, F. Lancon, and P. Pochet, *Thin Solid Films* **518**, 2422 (2010).

<sup>35</sup>A. Bongiorno and A. Pasquarello, *Appl. Phys. Lett.* **83**, 1417 (2003).

<sup>36</sup>A. A. Demkov and O. F. Sankey, *Phys. Rev. Lett.* **83**, 2038 (1999).

<sup>37</sup>R. M. Van Ginhoven and H. P. Hjalmarson, *Nucl. Instrum. Methods Phys. Res. B* **255**, 183 (2007).

<sup>38</sup>H. Ohta, T. Watanabe, and I. Ohdomari, *Phys. Rev. B* **78**, 155326 (2008).

<sup>39</sup>H. Ohta, T. Watanabe, and I. Ohdomari, *Jpn. J. Appl. Phys.* **46**(1), 3277 (2007).

<sup>40</sup>A. C. T. van Duin, A. Strachan, S. Stewman, Q. S. Zhang, X. Xu, and W. A. Goddard, *J. Phys. Chem. A* **107**, 3803 (2003).

<sup>41</sup>S. Plimpton, *J. Comput. Phys.* **117**, 1 (1995).

<sup>42</sup>J. C. Fogarty, H. M. Aktulga, A. Y. Grama, A. C. T. van Duin, and S. A. Pandit, *J. Chem. Phys.* **132**, 174704 (2010).

<sup>43</sup>P. Vashishta, R. K. Kalia, J. P. Rino, and I. Ebbsjo, *Phys. Rev. B* **41**, 12197 (1990).

<sup>44</sup>Y. J. Chabal, K. Raghavachari, X. Zhang, and E. Garfunkel, *Phys. Rev. B* **66**, 161315 (2002).

<sup>45</sup>A. Hemeryck, A. J. Mayne, N. Richard, A. Esteve, Y. J. Chabal, M. D. Rouhani, G. Dujardin, and G. Comtet, *J. Chem. Phys.* **126**, 114707 (2007).

<sup>46</sup>N. Richard, A. Esteve, and M. Djafari-Rouhani, *Comput. Mater. Sci.* **33**, 26 (2005).

<sup>47</sup>H. W. Yeom and R. Uhrberg, *Jpn. J. Appl. Phys.* **39**(1), 4460 (2000).

<sup>48</sup>A. Pasquarello, M. S. Hybertsen, and R. Car, *Phys. Rev. B* **53**, 10942 (1996).

<sup>49</sup>B. E. W. R. L. Mozzi, *J. Appl. Cryst.* **2**, 164 (1969).

<sup>50</sup>D. I. Grimley, A. C. Wright, and R. N. Sinclair, *J. Non-Cryst. Solids* **119**, 49 (1990).

<sup>51</sup>M. T. Yin and M. L. Cohen, *Phys. Rev. B* **26**, 5668 (1982).